

Supplemental information

Controlling mitochondrial membrane architecture via MIC60 determines viral replication to promote anti-viral immunity

Ichiro Katahira, Nina Liebrand, Michal Gorzkiewicz, Niklas Paul Klahm, Džiuljeta Abromavičiūtė, Julia Werner, Karina Stephanie Krings, Sarah Orywol, Tobias Lautwein, Karl Köhrer, Diran Herebian, Ertan Mayatepek, Max Anstötz, Ann Kathrin Bergmann, Arun Kumar Kondadi, Haifeng C. Xu, Aleksandra A. Pandyra, Takumi Kobayashi, Dirk Brenner, Thomas Floss, Ulrich Kalinke, Andreas S. Reichert, and Philipp A. Lang

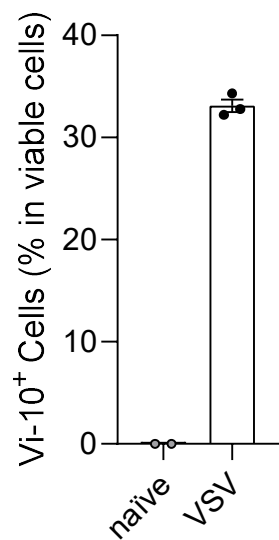
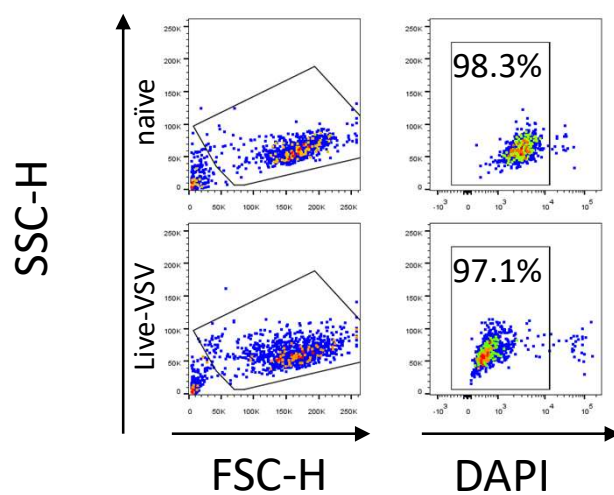
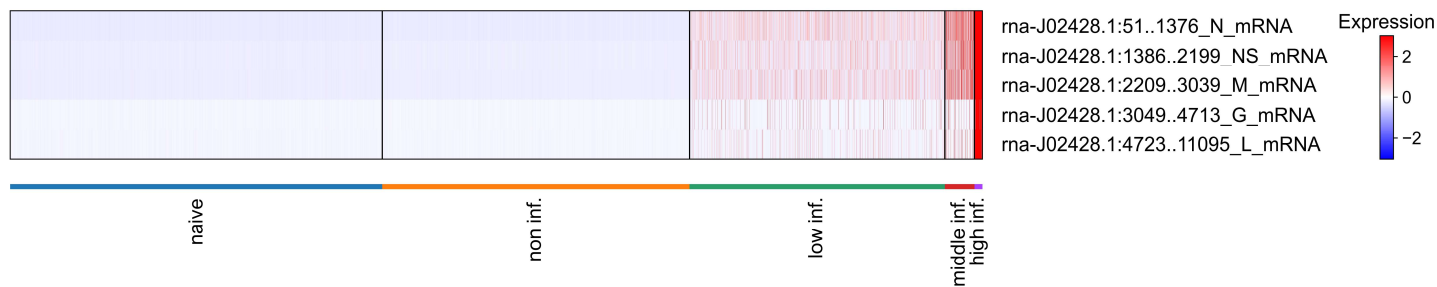
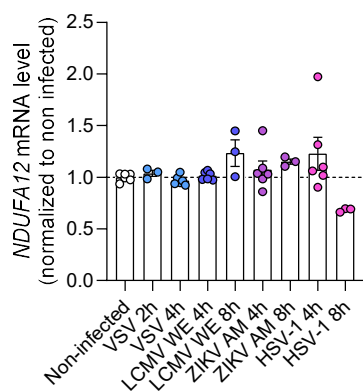
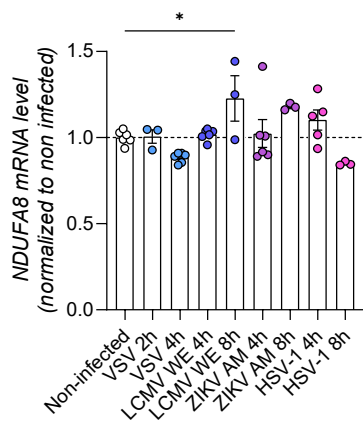
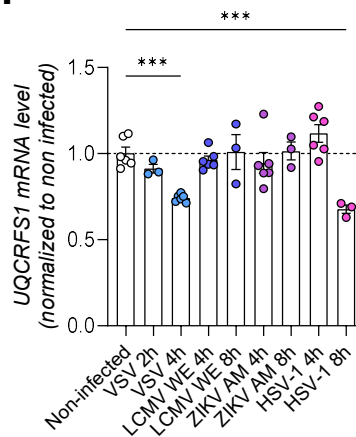
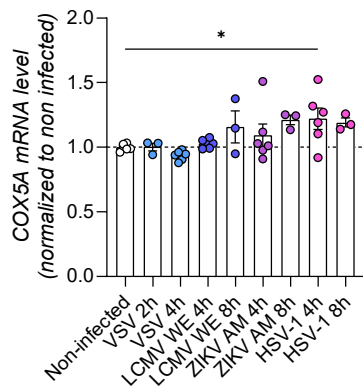
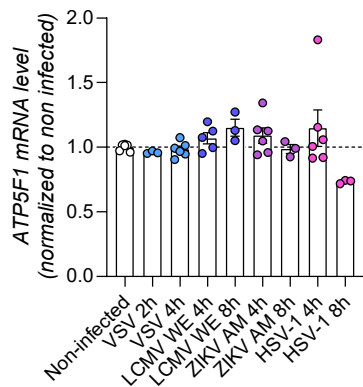
A**B****C****D****E****F****G****H**

Figure S1: Supplemental information for the single cell RNA sequencing and ETC gene expression after viral infection, related to Figure 1.

(A) VSV infected cells were stained with anti-VSV glycoprotein antibody (Vi-10) at 24h post-infection. HEK cells were infected with VSV as described in Figure 1A, and monensin was added at 4h post-infection to halt further viral propagation. The remaining cells of the samples for single cell RNA sequencing were used; n=2 for control, n=3 for VSV infected group.

(B) HEK cells were infected with VSV and viable cells were sorted as described in Figure 1A. Viability of the samples for single cell RNA sequencing was assessed after staining with DAPI.

(C) Heatmap showing expression of VSV transcripts in each cell.

(D-H) HEK cells were infected with VSV, LCMV, ZIKV and HSV at MOI=10, mRNA levels of (D) NDUFA12, (E) NDUFA8, (F) UQCRC1, (G) COX5A and (H) ATP5F1 were measured at the indicated time points; data were from two experiments for naïve and 4h post-infection, and one experiment for 2h and 8h post-infection. *p* values were determined using one-way ANOVA with Dunnett's multiple comparisons test. **p*<0.05, ****p*<0.001. Data are represented as mean ± S.E.M.

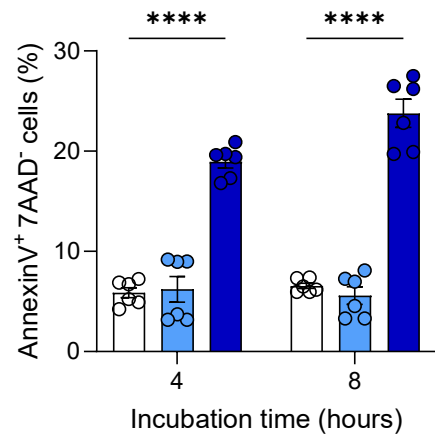
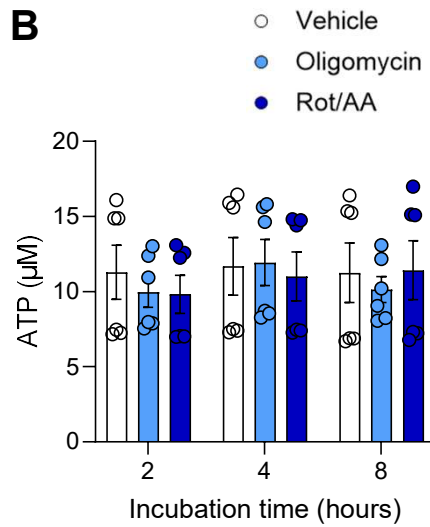
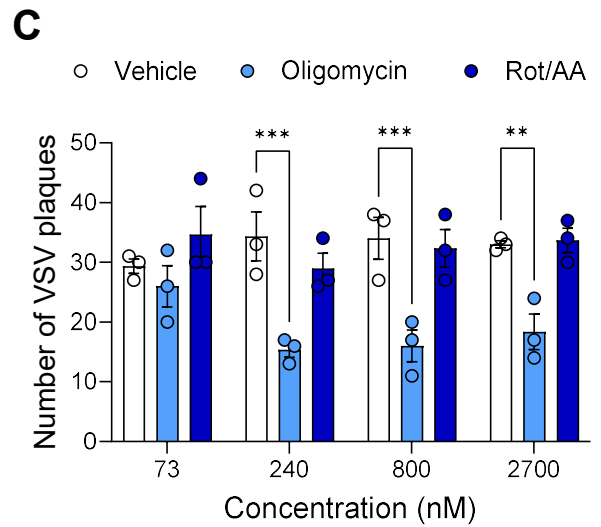
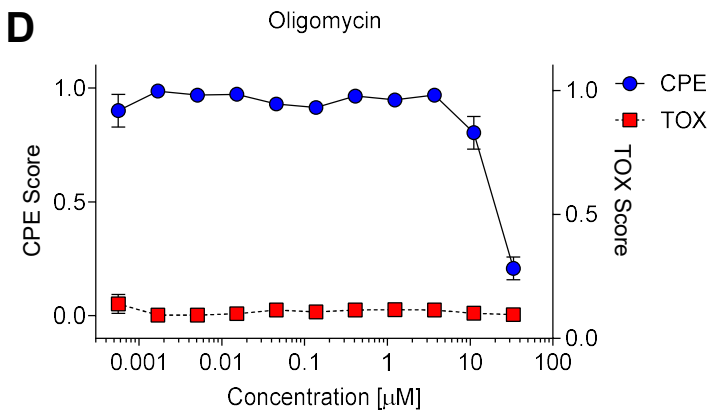
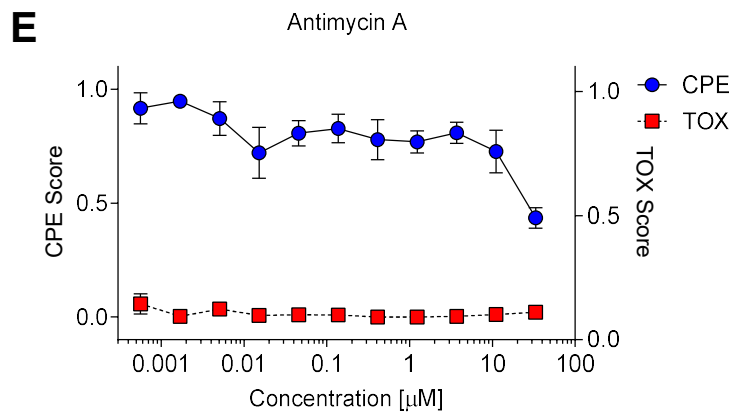
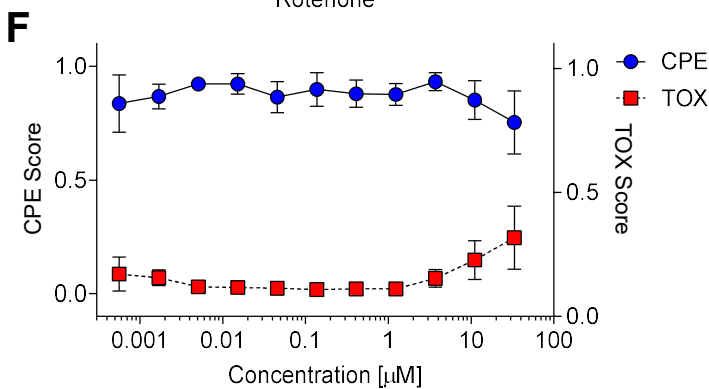
A**B****C****D****E****F**

Figure S2: Oligomycin treatment does not significantly affect early apoptosis or intracellular ATP level. Oligomycin inhibits VSV plaque formation and cytopathic effect of SARS-CoV-2, related to Figure 2.

(A) Vero cells were treated with 200 nM of oligomycin, 500 nM of rotenone and antimycin or DMSO for 4h or 8h. The treated cells were stained with annexin V and 7AAD; data from two independent experiments are shown. *p* values were determined using ordinary two-way ANOVA with Dunnett's multiple comparisons test. *****p*<0.0001. Data are represented as mean ± S.E.M.

(B) Vero cells were treated with 200 nM of oligomycin, 500 nM of rotenone and antimycin or DMSO for 2h, 4h or 8h. The treated cells were lysed after washing with PBS and ATP concentration was quantified with Luminescent ATP Detection Assay Kit; data from two independent experiments are shown. Statistical significance was determined by ordinary two-way ANOVA with Dunnett's multiple comparisons test. Data are represented as mean ± S.E.M.

(C) VSV plaque formation in Vero cells pre-treated with oligomycin, Rot/AA or vehicle; data were from one experiment pooled with n=3. *p* values were determined using ordinary two-way ANOVA with Dunnett's multiple comparisons test. ***p*<0.01, ****p*<0.001. Data are represented as mean ± S.E.M.

(D-F) Vero cells were treated with the indicated concentration of (D) oligomycin, (E) antimycin and (F) rotenone for 20 min prior to infection with SARS-CoV-2 at MOI of 0.03. Images were taken 3 days post-infection and CPE scores (blue) and TOX scores (red) were determined by 'CPETOXnet' and are shown in a concentration-dependent manner; data from two independent experiments are shown.

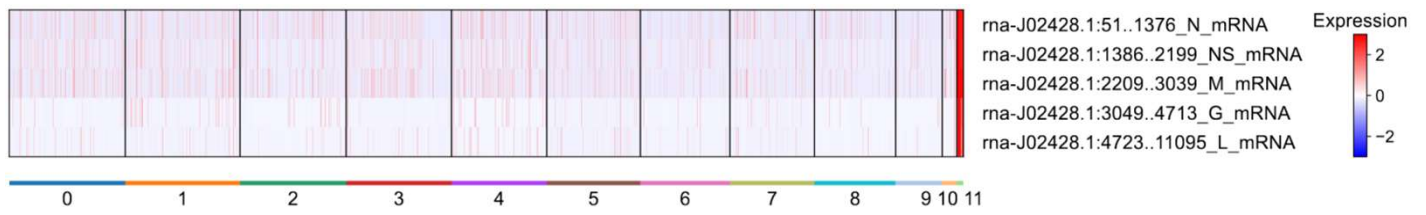
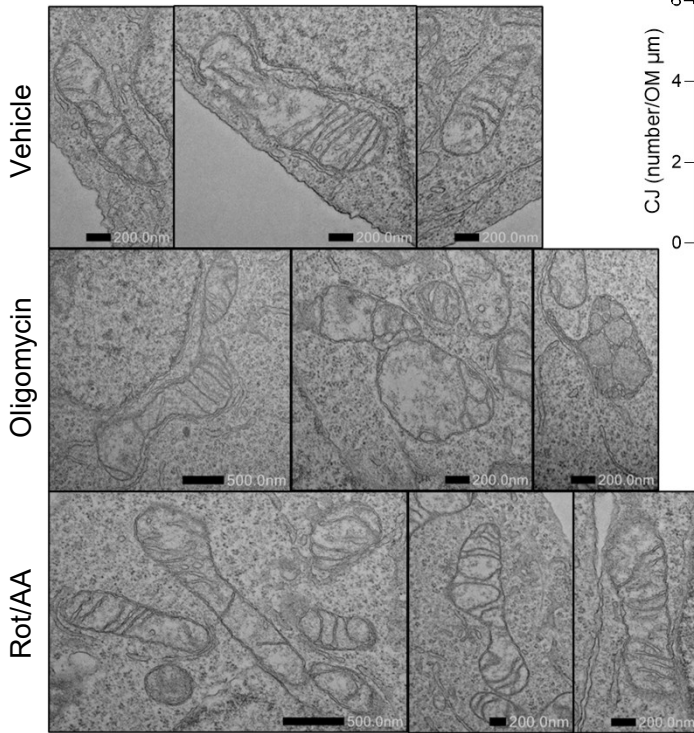
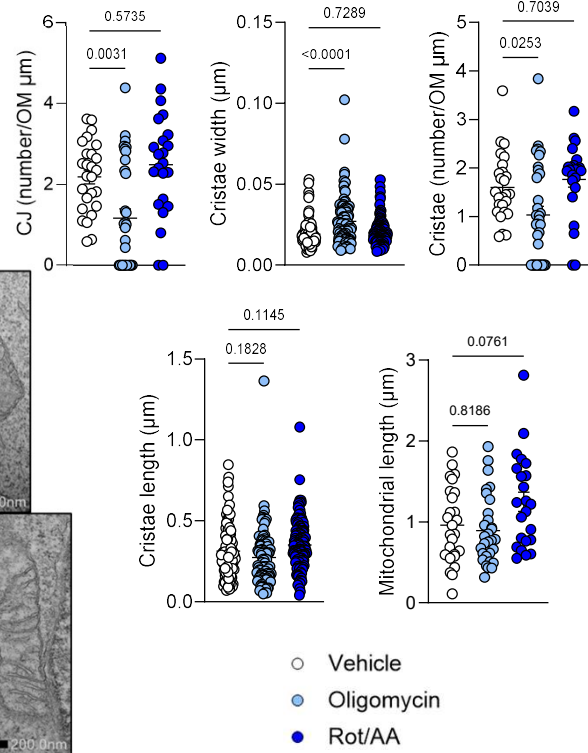
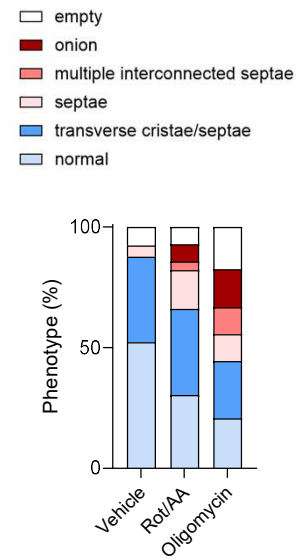
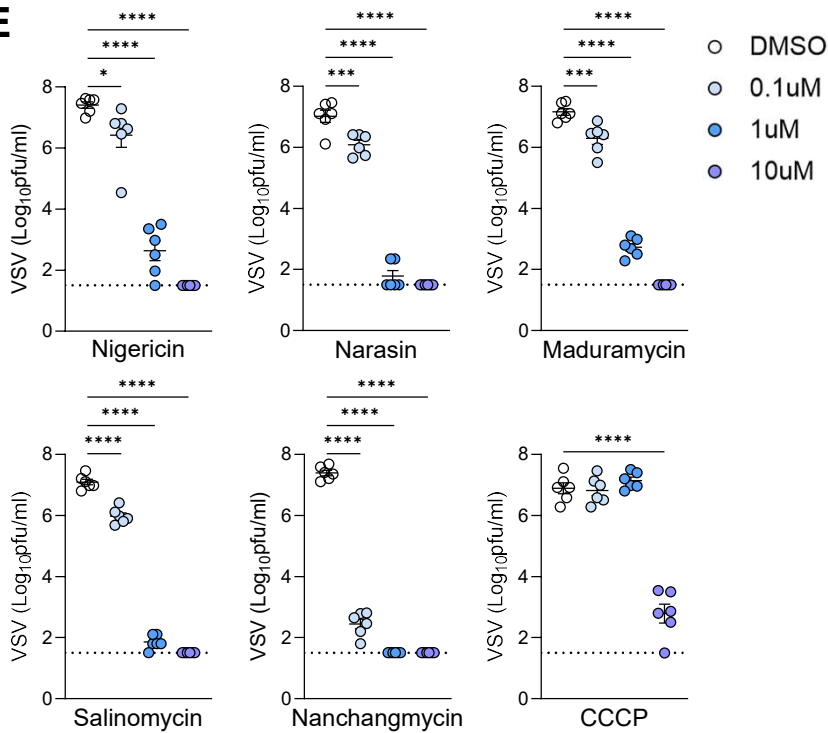
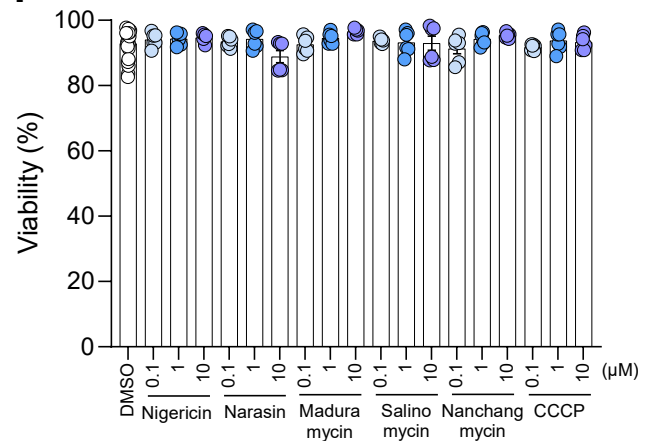
A**B****C****D****E****F**

Figure S3: Rot/AA treatment has only modest effect on cristae structure and mitochondrial morphology compared to oligomycin. Uncouplers reduce VSV replication without significantly affecting cell viability, related to Figure 3.

(A) Heatmap showing expression of VSV transcripts in each cell. The numbers at the bottom refer to the cluster numbers.

(B-D) HAP1 cells were treated with 200 nM of oligomycin, 500 nM of Rot/AA or vehicle for 8h. (B) Representative transmission electron microscopy (TEM) micrographs. Scale bar lengths are specified individually on each image: the scale bar in the left panel of oligomycin and Rot/AA represents 500nm, while all other scale bars indicate 200nm. (C) Quantification of TEM micrographs: number of crista junction, cristae length, cristae width, number of cristae and mitochondrial length were analyzed; 23-30 mitochondria per condition were analyzed. Statistical significance was determined using one-way ANOVA with Dunnett's multiple comparisons test. Data are represented as mean \pm S.E.M. (D) Mitochondria were classified based on morphological phenotype and relative abundance is shown; 56-65 mitochondria per condition were analysed.

(E) Vero cells were infected with VSV at MOI=0.001 after the pre-treatment with the indicated uncouplers for 30 min. VSV titers in the supernatant were quantified at 16h post-infection; data are representative of two independent experiments. p values were determined using one-way ANOVA with Dunnett's multiple comparisons test. * p <0.05, *** p <0.001, **** p <0.0001. Data are represented as mean \pm S.E.M.

(F) Vero cells were treated with the compounds at the indicated concentrations for 16 hours. The relative abundance of annexin V-/ 7AAD⁻ cells is shown as viability: data are representative of two experiments. Statistical significance was determined by one-way ANOVA with Dunnett's multiple comparisons test. Data are represented as mean \pm S.E.M.

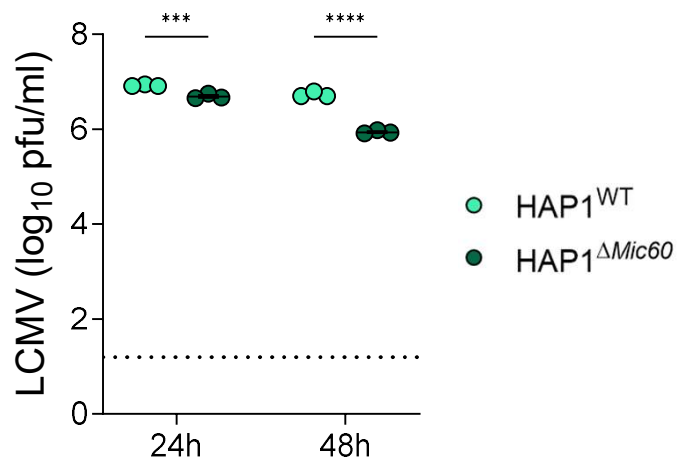
A

Figure S4: LCMV replication is reduced in MIC60 deficient HAP1 cells, related to Figure 4.

(A) WT and MIC60-deficient HAP1 cells were infected with LCMV WE at MOI=1. LCMV titer in the infected supernatant was measured at the indicated time points; data from one experiment pooled with n=3 per condition are shown. Significance was determined using ordinary two-way ANOVA followed by Sidak's multiple comparisons test. *** $p < 0.001$, **** $p < 0.0001$. Data are represented as mean \pm S.E.M.

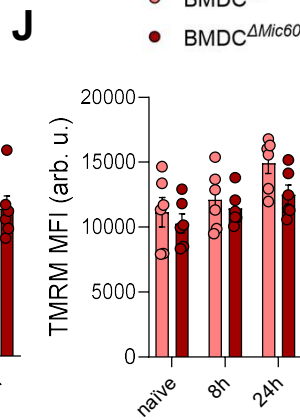
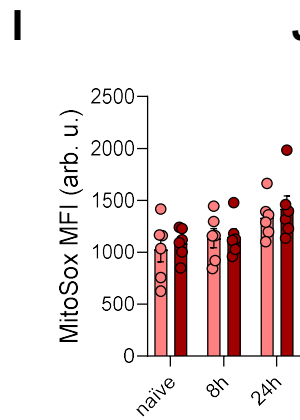
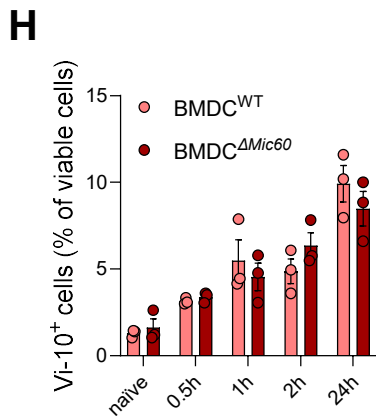
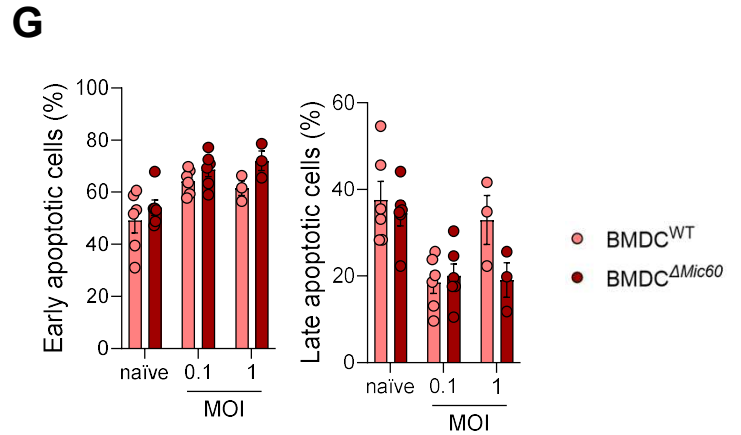
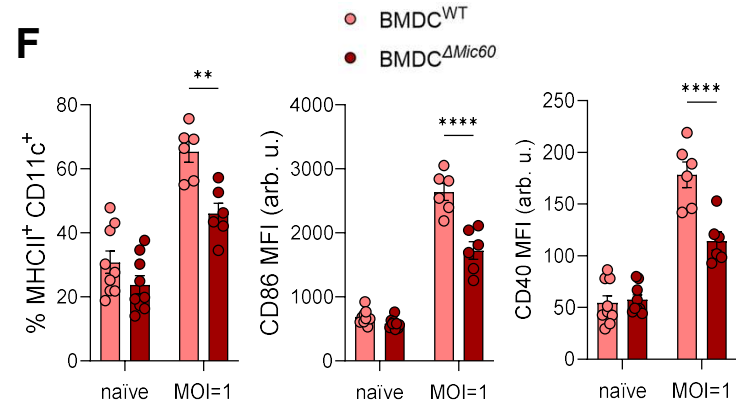
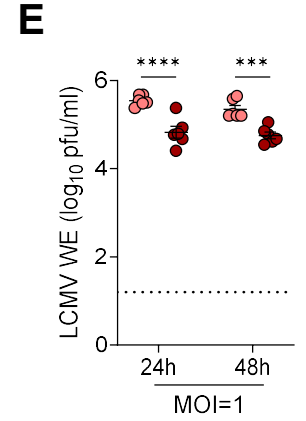
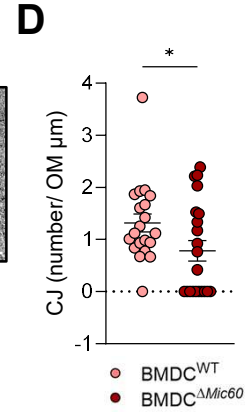
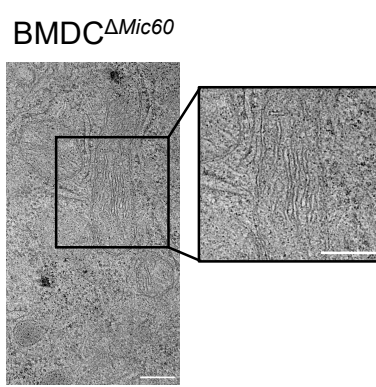
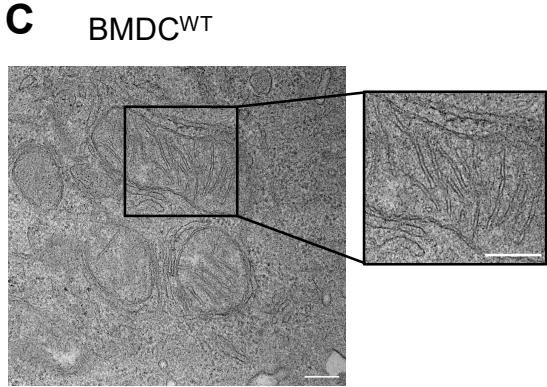
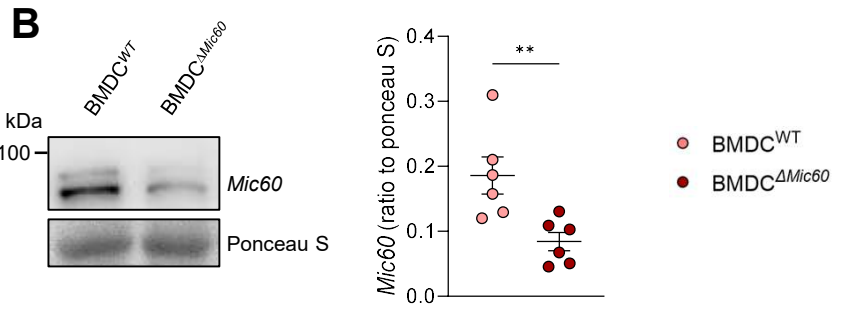
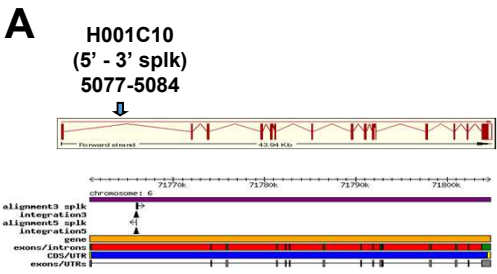


Figure S5: Supplemental information for generation of *Mic60*^{inv/inv} × *CD11c-Cre*⁺ mice, and characterization of MIC60 deficient BMDCs, related to Figure 5.

(A) Schematics of IMMT^{GT(H001C10)WRST}:MGI:3897023, where the gene trap had inserted in the intron 1 of the *Mic60* (*IMMT*) gene locus.

(B) MIC60 expression in BMDCs from WT or *Mic60*^{inv/inv} × *CD11c-Cre*⁺ mice; data from two independent experiments pooled with n=6 mice per condition are shown. Significance was determined using two-tailed/unpaired Student's t-test. ***p*<0.01. Data are represented as mean ± S.E.M.

(C) Representative TEM micrographs of MIC60-deficient and competent BMDCs and (D) quantification of CJs; scale bar 200 nm, data from two experiments pooled with n=2 mice per condition. Significance was determined by two-tailed/unpaired Student's t-test. **p*<0.05. Data are represented as mean ± S.E.M.

(E) MIC60-deficient and competent BMDCs were infected with LCMV WE strain at MOI=1. LCMV titer in the infected supernatant was measured at the indicated time points; data from two independent experiments pooled with n=6 mice. *p* values were determined using ordinary two-way ANOVA followed by Sidak's multiple comparisons test. ****p*<0.001, *****p*<0.0001. Data are represented as mean ± S.E.M.

(F) Statistics of CD11c⁺MHC-II⁺ BMDCs, MFI of CD86 and CD40 related to Figure 5G-I; data from three experiments pooled with n=9 mice for naïve condition and two experiments pooled with n=6 mice for infected condition. Significance was determined using ordinary two-way ANOVA followed by Sidak's multiple comparisons test. ***p*<0.01, *****p*<0.0001. Data are represented as mean ± S.E.M.

(G) BMDCs were infected with VSV at indicated MOI and the cells were stained with annexin V and 7AAD at 24h post-infection; data are representative of six biological replicates for naïve and MOI=0.1 and three biological replicates for MOI=1 condition. Significance was analyzed using ordinary two-way ANOVA followed by Sidak's multiple comparisons test. Data are represented as mean ± S.E.M.

(H) BMDCs were infected with VSV at MOI=1 and monensin was added at indicated time points to halt further entry of viral particles. The cells were stained with Vi-10 at 24h post-infection; data represent three biological replicates. Significance was analyzed by ordinary two-way ANOVA followed by Sidak's multiple comparisons test. Data are represented as mean ± S.E.M.

(I-J) BMDCs were infected with VSV at MOI=0.1 and at 8 and 24h post-infection, the cells were stained with (I) MitoSox and (J) TMRM; data were from two independent experiments pooled with n=6 mice. Statistical significance was analyzed using ordinary two-way ANOVA followed by Sidak's multiple comparisons test. Data are represented as mean ± S.E.M.

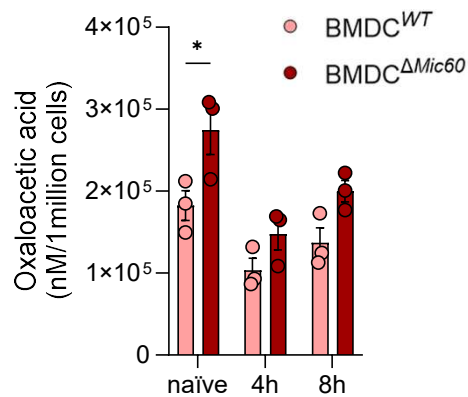
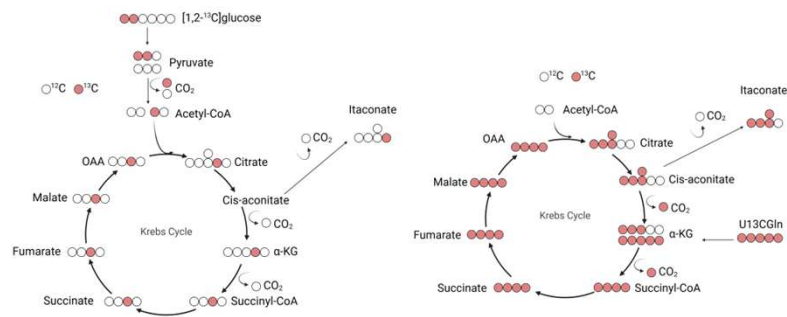
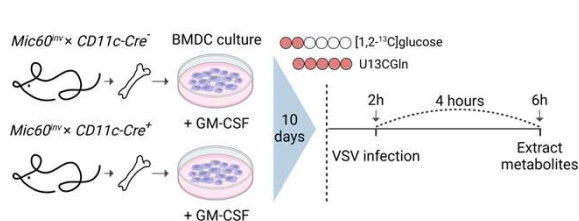
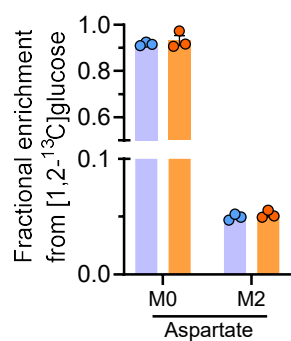
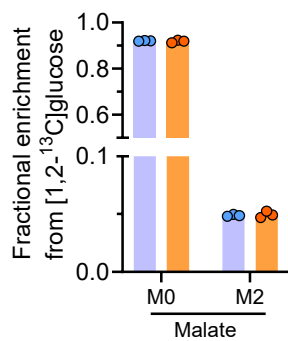
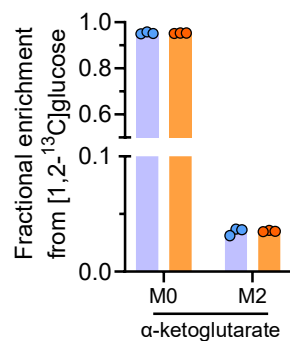
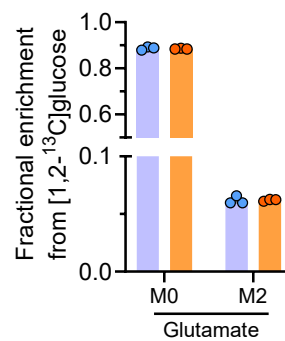
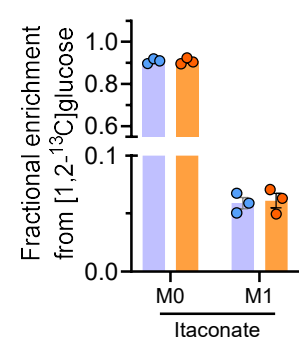
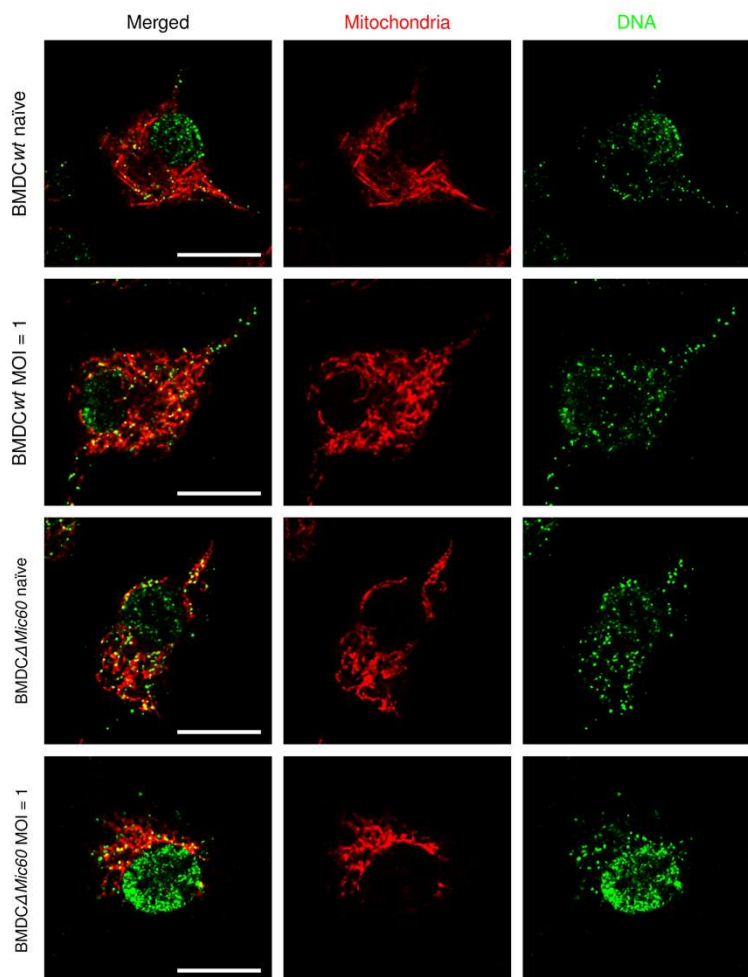
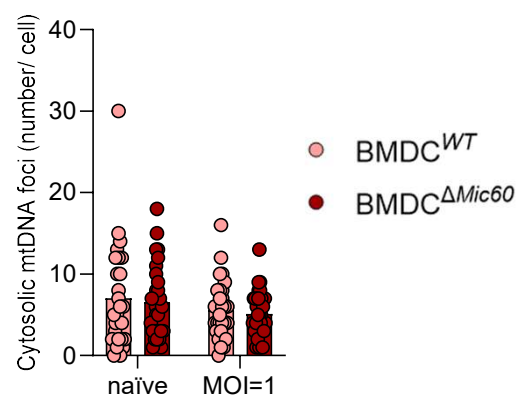
A**B****C****D****E****F****G****H****I****J**

Figure S6: Metabolic flux analysis and cytosolic mtDNA quantification in MIC60-competent or deficient BMDCs, related to Figure 6

(A) statistics of oxaloacetic acid concentration in MIC60-competent or deficient BMDCs, related to Figure 6E; data are representative of three biological replicates. Significance was determined using ordinary two-way ANOVA followed by Sidak's multiple comparisons test. * $p < 0.05$. Data are represented as mean \pm S.E.M.

(B) Fluxmap of mammalian central carbon metabolism; illustration was created with Biorender.com.

(C) Schematic depicting experimental procedures of metabolic flux analysis in BMDCs; illustration was made with Biorender.com.

(D-H) MIDs (mass isotopomer distributions) of (D) aspartate, (E) malate, (F) α -ketoglutarate, (G) glutamate and (H) itaconate from MIC60-competent or deficient BMDCs that were incubated with [1,2- ^{13}C] glucose; data are representative of three biological replicates. Data are represented as mean \pm S.E.M.

(I-J) Quantification of cytosol DNA foci released from mitochondria. BMDCs were infected with VSV at MOI=1 for 4h. Cytosolic DNA foci were counted manually when cytosolic DNA foci are not co-localized with mitochondria; scale bar 10 μm , data are representative of three biological replicates, 30 cells per condition were analyzed except naïve WT BMDCs (27 cells). Statistical significance was analyzed using ordinary two-way ANOVA followed by Sidak's multiple comparisons test. Data are represented as mean \pm S.E.M.

Table S1: Primers for real-time quantitative PCR

Gene	Forward Primer	Reverse Primer
VSV glycoprotein	5'-ACGGCGTACTTCCAGATGG-3'	5'-CTCGGTTCAAGATCCAGGT-3'
Gapdh mouse	5'-ACAAC TTTGGTATCGTGGAAGG-3'	5'-GCCATCACGCCACAGTTTC-3'
Ifnb1 mouse	5'-CAGCTCCAAGAAAGGACGAAC-3'	5'-GGCAGTGTA ACTCTTCTGCAT-3'
Ifna4 mouse	5'-TGATGAGCTACTACTGGTCAGC-3'	5'-GATCTCTTAGCACAAAGGATGGC-3'
Cxcl10 mouse	5'-CCAAGTGCTGCCGTCATTTTC-3'	5'-GGCTCGCAGGGATGATTCAA-3'
ND6 human	5'-GCGATGGCTATTGAGGAGTATCC-3'	5'-CACAGCACCAATCCTACCTCCA-3'
MT-CO1 human	5'-TCTCAGGCTACACCCTAGACCA-3'	5'-ATCGGGGTAGTCCGAGTAACGT-3'
Mx1 mouse	5'-GACCATAGGGGTCTTGACCAA-3'	5'-AGACTTGCTCTTTCTGAAAAGCC-3'
Ifit2 mouse	5'-AGTACAACGAGTAAGGAGTCACT-3'	5'-AGGCCAGTATGTTGCACATGG-3'
Ifit3 mouse	5'-CCTACATAAAGCACCTAGATGGC-3'	5'-ATGTGATAGTAGATCCAGGCGT-3'
NDUFA12 human	5'-GGTCTCCGAGGCTATCTACGG-3'	5'-GGAGGCACCATGCTTCCATC-3'
NDUFA8 human	5'-CCCAACAAGGAGTTTATGCTCT-3'	5'-CACAGTGACGTTTTATCTGCCT-3'
UQC RFS1 human	5'-CTGAATACCGCCGCCTTGAA-3'	5'-ATGCGACACCCACAGTAGTTA-3'
COX5A human	5'-ATCCAGTCAGTTCGCTGCTAT-3'	5'-CCAGGCATCTATATCTGGCTTG-3'
ATP5F1 human	5'-AGGTCCAGGGGTATTGCAG-3'	5'-TCCTCAGGGATCAGTCCATAAC-3'